 CMC, vol.7, no.3, pp.167-189, 2008

Computational Studies on Mechanical and Thermal Properties of Carbon Nanotube Based Nanostructures

Arnab Chakrabarty[1] **and Tahir Çağin**[1]

Abstract: The excellent set of properties of carbon nanotube and carbon nanotube-based nanostructures has been established by various studies. However the claimed property values and trends have not been unanimously agreed upon. Using state of the art molecular dynamics and ab initio methods, we have extensively studied the mechanical, thermal and structural properties of carbon nanotubes and carbon nanotube based nanostructures. Additionally this study aims to address the approaches used in various studies to assess the validity and influence of various definitions used for determining the physical properties as reported in earlier experiments and theoretical calculations. We have come up with equations, which quantitatively address the wide differences in trend and values of nanotube axial modulus available across the literature. Applying a novel bond rearrangement scheme, we have found similar values in twist modulus of zigzag and armchair nanotubes. This opposes the claim of difference that was shown to be valid only at finite limit in our study. We have shown that the contribution of van der Waals energy in a multi-wall nanotube is powerful enough to make it hexagonal in shape but negligible in affecting the axial modulus. These insights will also help in designing micromechanics model of materials made from carbon nanotube or nanotube like structures. In particular, we have calculated the mechanical properties (young modulus, bending modulus and twist modulus) of isolated and bundled nanotubes, single and multi-wall nanotubes and single and multi-wall carbon nanotube based tori. We also report studies on thermal variation of moduli and thermal expansion of nanotubes. The result obtained by first principles calculation based interatomic potential agrees well with the experimental results.

[1] Texas A&M University, Artie McFerrin Department of Chemical Engineering, 519 Jack E. Brown Engineering Building, 3122 TAMU, College Station, TX 77843-3122

1 Introduction

The plethora of definitions, procedures, techniques, instruments, theories or the lack of these has established the superiority of nanotubes. However they also have raised questions for the values observed, claimed trends and their dependence on variation of external parameters. For instance, the elastic modulus of carbon nanotube has been calculated and measured by various approaches, ranging from values of several hundred GPa (Yakobson, Brabec et al. 1996; Cornwell and Wille 1997; Lu 1997; Gao, Cagin et al. 1998; Salvetat, Briggs et al. 1999; Zhou, Duan et al. 2001) few (Y>=1) TPa (Treacy, Ebbesen et al. 1996; Krishnan, Dujardin et al. 1998; Alford, Landis et al. 2005; Enomoto, Kitakata et al. 2006) to as high as 5.5 TPa (Yakobson, Brabec et al. 1996). A brief inspection of Figure 1 and Table 1 gives a rough idea of the scattered nature of the data available.

Apart from values, trends like variation of the modulus with respect to the tube diameter also shows conflicts (Cornwell and Wille 1997; Pop, Mann et al. 2006). In evaluations of thermal transport properties, we encounter values of thermal conductivity reported as low as $\sim$ 30 W/cm-K (Che, Cagin et al. 2000; Pop, Mann et al. 2006) and as high as $\sim$ 600 W/cm-K (Berber, Kwon et al. 2000; Klemens 2001), representing a factor of 20 discrepancy. This difference is similar to the scatter observed in evaluation of mechanical properties. Results reported on the thermal expansion of coefficients of nanotubes are not free of debate either. Promising technological application potential for carbon nanotubes, hence, has re-

Table 1: Axial elastic modulus of single-wall isolated carbon nanotubes.

Reference	Tensile Modulus	Method
(Cornwell and Wille 1997)	650 GPa (10, 10)	MD simulation using Tersoff - Brenner potential near 0 K. T < 0.005 K
(Van Lier, Van Alsenoy et al. 2000)	$\sim$ 1TPa (5, 5) and (9, 0)	*ab initio* Hartree-Fock 6-31 G basis set
(Popov, Van Doren et al. 2000)	$\frac{\partial^2 E}{\partial \varepsilon^2} = 55eV$	Lattice dynamical model Born perturbation technique was used to derive analytical expression of sound velocities
(Gao, Cagin et al. 1998)	640 GPa	Molecular mechanics. Second derivative of energy with respect to strain
(Lu 1997)	563 GPa	Empirical force constant model. Second derivatives of energy, with respect to strain.
(Chang and Gao 2003)	$\sim$ 1TPa	Analytical model based on molecular mechanics approach. Force constants obtained from experimental data of graphite.
(Sanchez-Portal, Artacho et al. 1999)	$\frac{\partial^2 E}{\partial \varepsilon^2} = 52eV$ (10, 10)	DFT calculation with LDA approximation.
(Reich, Thomsen et al. 2002)	930 GPa (d = 14 A)	First principle calculations, using LDA in DFT.
(Treacy, Ebbesen et al. 1996)	1.8 TPa (average of 11 samples)	Measuring amplitude of intrinsic thermal vibrations by Transmission electron microscope (TEM)
(Alford, Landis et al. 2005)	1.06 TPa	LDA approach based on LCGTO.
(Xiao, Gama et al. 2005)	$\sim$ 1TPa	Structural mechanics model for defect free model SWNT. Modified Morse potential has been used.
(Krishnan, Dujardin et al. 1998)	1.25 TPa (average over 27 SWNT)	Measuring amplitude of intrinsic thermal vibrations by Transmission electron microscope (TEM)
(Cai, Bie et al. 2004)	0.95 TPa (5, 0) SWNT	Using Tersoff Brenner potential developed by from DFT. Second derivative of energy.
(Yakobson, Brabec et al. 1996)	5.5 TPa $\frac{\partial^2 E}{\partial \varepsilon^2} = 59eV$	Molecular mechanics using Tersoff Brenner potential
(Salvetat, Briggs et al. 1999)	0.81 TPa	Through exerting load by AFM on suspended nanotube
(Lourie and Wagner 1998)	2.8-3.6 TPa	Micro Raman Spectroscopy

sulted in an exponentially increasing research reports (Figure 2). It also has created the necessity for sifting through these inconsistencies in intrinsic property values and have a clear understanding of addressing these properties.

The theoretical methods(Shen and Atluri 2004) used to evaluate the elastic modulus of CNT include, but are not limited to, first principles(Sanchez-Portal, Artacho et al. 1999; Reich, Thomsen et al. 2002) classical molecular dynamics(Cornwell and Wille 1997), classical molecular mechanics (Gao, Cagin et al. 1998), empirical force constants model(Lu 1997) and structural mechanics models(Xiao, Gama et al. 2005). Multi-walled carbon nanotube has been modeled as multiple elastic cylindrical structures to find the characteristics of wave (Xie, Han et al. 2007). Vibration behavior using micropolar

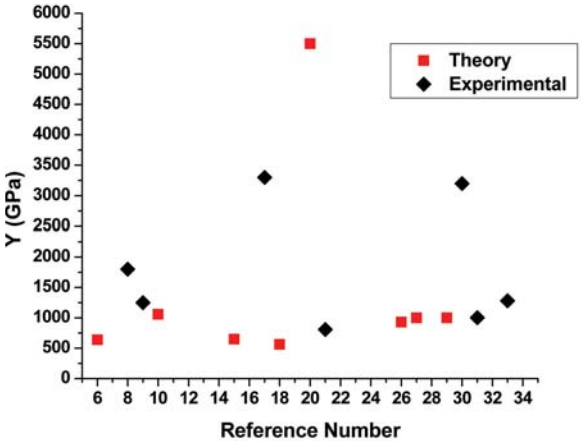

Figure 1: The Young modulus values reported in 14 different references (theory and experiments are plotted together, to indicate the scatter mentioned in the text exist in both) for CNT. The x-axis numbering corresponds to the sequence in our citation.

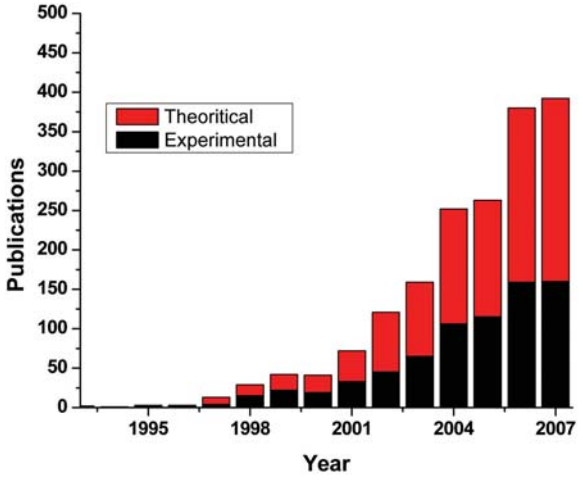

Figure 2: Number of articles over the past decade on properties of carbon nanotubes, generated using the data from ISI Web of Science database obtained by a set of appropriate keyword search (it is not meant to be comprehensive).

theory has shown a decrease in fundamental frequency with increase in aspect ratio (Xie and Long 2006). Molecular mechanics based finite element modeling has been done on carbon nanotube using semi-empirical Brenner potential (Theodosiou and Saravanos 2007). The potential energy functions used to model the interactions of atoms, includes Tersoff-Brenner potentials (Cornwell and Wille 1997; Cai, Bie et al. 2004), force fields developed from ab-initio calculations of graphite (Gao, Cagin et al. 1998) or force fields developed based on the experimental results of graphite (Chang and Gao 2003). First principle calculations also come with different flavors. Most common ones are the use of methods based on Hartree Fock theory (Van Lier, Van Alsenoy et al. 2000) or the density functional theory (Sanchez-Portal, Artacho et al. 1999; Reich, Thomsen et al. 2002). Experiments which explored the mechanical properties of nanotubes include the use of transmission electron microscope (Treacy, Ebbesen et al. 1996; Krishnan, Dujardin et al. 1998; Enomoto, Kitakata et al. 2006), atomic force microscope (Salvetat, Briggs et al. 1999), micro Raman spectroscopy (Lourie and Wagner 1998) and scanning electron microscope (Yu, Files et al. 2000). Furthermore, mechanical resonance method (Treacy, Ebbesen et al. 1996; Krishnan, Dujardin et al. 1998), scanning force microscopy method (Wong, Sheehan et al. 1997; Falvo, Clary et al. 1998), nanomanipulation (Yu, Files et al. 2000) are some of the different methods used by the researchers in experiments for nanotube property estimation. Quite a few review papers (Thostenson, Ren et al. 2001; Yakobson and Avouris 2001; Dong, Gregory et al. 2002; Srivastava, Wei et al. 2003; Dresselhaus, Dresselhaus et al. 2004; Ashrafi and Hubert 2006) have presented useful discussions on carbon nanotubes, their intrinsic properties, and their determination from theory and experimental characterization methods. There are suggestions that attribute the variation of properties of nanotubes to factors like purity of tubes, orientation, misalignment, etc. in experiments. In theory, one can identify the use of different definitions as a possible source of scatter in properties.

In the following we have presented our findings on mechanical and thermal properties of carbon nanotube and nanotube like structures to get further insight and address the existing discrepancies. We assess the applicability of different definitions and show that a major part of the discrep-

ancies have arisen from different ways of dealing with the continuum theories at the nanoscale level.

We first present the model systems used in these simulations, followed by a description of the methods and procedures used in this study. We then present the results of our calculations on thermo mechanical properties of isolated single-wall carbon nanotubes, single-wall carbon nanotube bundles, multi-wall carbon nanotubes, single and multi-wall carbon nanotube based tori. We finally comment and derive conclusions from these computational experiments on the properties of carbon nanotube.

2 Model Systems and Computational Methods

2.1 Model Systems

Most of our studies were conducted on single-wall carbon nanotubes both in isolated and bundled forms, either infinite or finite lengths. We have constructed model with different radii and chirality for a given (n, m)-pair. We have furthermore conducted studies on multi-wall carbon nanotubes mostly based on concentric (n, n) armchair tubes, having interlayer spacing as $\sim$ 3.4 A, implying any double wall armchair CNT is to be made from (n, n) and (n+5, n+5) tubes. In addition to the straight nanotubes we also conducted extended study on single-wall and multi-wall carbon nanotube based tori structure as they are good structures to explore bending modulus of carbon nanotube based nanostructures.

2.2 Computational Methods

We have used three main methods in our work: ab-initio methods based molecular mechanics; classical force field based molecular mechanics and classical molecular dynamics simulation.

The *ab initio* calculations have been performed in the general framework of DFT (Hohenberg and Kohn 1964; Kohn and Sham 1965; Payne, Teter et al. 1992) using projector augmented wave method (PAW) (Kresse and Joubert 1999) with the generalized gradient approximation (GGA). To account for the exchange correlation we employed the exchange-correlation function due to Perdew-Burke-Ernzerhof (PBE) (Perdew, Burke et al. 1996). Kinetic energy cutoff of the electronic wave functions was taken as 600 eV. Integrals over the Brillouin zone were summed on a Monkhorst-Pack mesh (Monkhorst and Paack 1976) of 8x8x8 unless otherwise stated.

In molecular mechanics method we have used the force field described in section 2.3. For structural optimization (atomic positions and cell parameters) through minimization of energy we have used conjugate gradient method. We fitted the strain energy with respect to deformation and estimated the value of second derivative of energy with respect to the strain variables. This yields the values of the elastic constants on the basis of the following Taylor series expansion of the energy E in terms of strain ε,

$$E(\varepsilon) = E_0 + \sum_{i=1}^{6} \left.\frac{\partial E}{\partial \varepsilon_i}\right|_0 \varepsilon_i + \frac{1}{2} \sum_{i,j=1}^{6} \left.\frac{\partial^2 E}{\partial \varepsilon_i \partial \varepsilon_j}\right|_0 \varepsilon_i \varepsilon_{j+\ldots} \tag{1}$$

Here E_0 refers to the energy of the zero-strain equilibrium configuration. Hence, one can determine the value of elastic constants by calculating $\frac{\partial^2 E}{\partial \varepsilon_i \partial \varepsilon_j}$ provided that the higher order terms are negligibly small due to applied small strains.

Molecular dynamics simulations were performed under two different ensembles. For constant-strain states we have used canonical ensemble (NVT) and for constant stress simulations we have employed constant pressure and constant temperature (NPT) ensemble methods. In either case equations of motion for atoms, Nose-Hoover thermostat variable and the cell variables are iteratively solved to follow the trajectory of the model system. Hence, we trace the dynamical evolution the model systems under given constraints. By keeping track of the microscopic properties of the system with respect to time, we can evaluate different dynamic and equilibrium properties of the system. Unless otherwise specified, the time step used for all the molecular dynamics run was chosen to be 1 femto-second (fs). Leapfrog Verlet algorithm was used for the integration of equations of motion.

2.3 Force Field

In classical mechanics based calculations (molecular mechanics and molecular dynamics), the potential energy of a system is represented by analytical functions, namely the interaction force fields. The parameters of these functions are optimized so as to reproduce the fundamental properties, density, lattice parameters, vibrational frequencies and the like. The functional forms are based on quantum mechanical arguments (Exp-6 form for van der Waals interactions, Morse form for bond stretch and harmonic form for angle bending, periodic truncated Fourier series forms for torsion). Hence, a force field is the mathematical expression that describes the dependence of potential energy of a molecular system to that of the atomic positions of its constituent atoms. The energy of a system can then be written as:

$$E = E_{VAL} + E_{NB} \tag{2}$$

$$E_{VAL} = E_B + E_A + E_T + E_I \tag{3}$$

$$E_{NB} = E_{VDW} + E_C \tag{4}$$

where:

E = Total energy of the system
E_{VAL} = Energy due to bonded interaction
E_{NB} = Energy due to non-bonded interaction
E_B = Energy due to Bond stretching (two body)
E_A = Energy due to angle bending (three body)
E_T = Energy due to torsion (four body)
E_I = Energy due to out of plane configuration (four body) or dihedral
E_{VDW} = Energy due to van der Waals interaction
E_C = Energy due to Columb interaction.

In this particular work the force field used for all the molecular dynamics and molecular mechanics calculation was derived from ab-initio calculation of graphite (Cagin, Gao et al. 2006). The contribution of different components of the total energy was computed as follows:
van der Waals Interaction:

$$E_{vdw} = D_{vdw}(\rho^{-12} - \rho^{-6}) \tag{5}$$

Where $\rho = r/r_v$, r_v being the separation at minimum energy between the two atoms.

Bond stretch energy:

$$E_{bond} = D_b(\chi - 1)^2 \tag{6}$$

Where $\chi = e^{-\gamma(r-r_b)}$ with r_b being the equilibrium bond distance.
Angle bending energy:

$$\begin{aligned} E_{angle} = {} & \frac{1}{2}k_\theta(\cos\theta - \cos\theta_a)^2 \\ & + k_{1\theta}(r_1 - r_{1\theta})(\cos\theta - \cos\theta_a) \\ & + k_{2\theta}(r_2 - r_{2\theta})(\cos\theta - \cos\theta_a) \\ & + k_{12}(r_1 - r_{1\theta})(r_2 - r_{2\theta}) \end{aligned} \tag{7}$$

where k_θ, $k_{x\theta}$, $k_{y\theta}$ and k_{xy} are the bond stretch and stretch-bend force constants.
Dihedral energy:

$$E_{dihedral}(\phi) = V_0 + V_1\cos\phi + V_2\cos(2\phi) \tag{8}$$

where V_0, V_1 and V_2 are expansion coefficients for the truncated Fourier expansion up to second order. The details of the force field parameter values are given elsewhere (Cagin, Gao et al. 2006).

3 Mechanical Properties of Carbon Nanotubes

3.1 Elastic Modulus of Carbon Nanotubes

In solid mechanics, Young's modulus or Elastic modulus gives a measure of the stiffness of a material. It is defined by

$$E = \frac{Stress}{Strain} = \frac{\sigma}{\varepsilon} = \frac{F/A_0}{\Delta l/l_0} \tag{9}$$

This definition is used to find the elastic modulus from molecular dynamics simulation of a system. We can also determine the full elastic stiffness matrix by applying the formal definition in Voigt notation:

$$C_{ij} = \frac{1}{V_0}\frac{\partial^2 E}{\partial\varepsilon_i\partial\varepsilon_j}, \quad i,j = 1,\ldots,6. \tag{10}$$

Single-wall Nanotube: We performed molecular mechanics calculations on carbon nanotube structures, by applying strain to the model system. For each fixed strain state, the atomic positions were optimized and corresponding strain energy

was evaluated. Subsequently, by using the second derivative of potential energy, we estimated the corresponding axial elastic constant. In the bundle calculations the cross sectional area was evaluated in a similar way as in reference (Gao, Cagin et al. 1998). Figure 3 shows variation of strain energy as a function of strain and associated fitting.

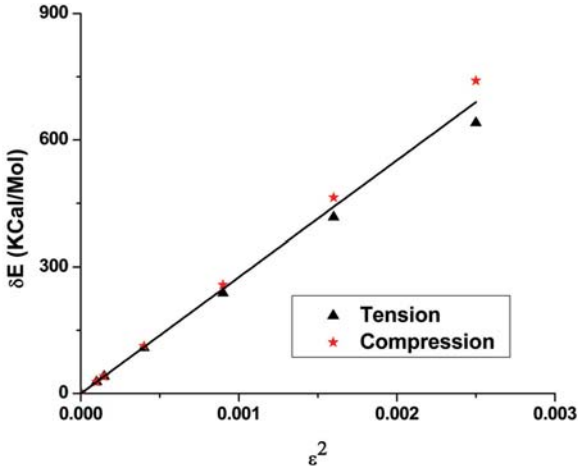

Figure 3: Strain energy content for tensile and compressive strains obtained from Molecular Mechanics calculations to determine the elastic modulus.

Validity of Force Field: Some of the disagreement between our work and the values found in literature lead us to calculate the axial modulus through DFT and reinforce our confidence on using graphite based force fields on carbon nanotubes. These calculations were carried out with a plane wave basis set. The axial modulus of a (10, 10) SWNT bundle from the second derivative of the energy was estimated to be 605 GPa. The value of second derivative of the energy with respect to strain, $\frac{\partial^2 E}{\partial \varepsilon^2}$, was found to have a value of 56.8 eV/atom, which compared well to values in literature (Robertson, Brenner et al. 1992; Sanchez-Portal, Artacho et al. 1999; Popov, Van Doren et al. 2000; Dresselhaus, Dresselhaus et al. 2001). This agreement rules out the possibility of force field being the source of any sort of discrepancy. Furthermore, it was accepted that the force field used to calculate SWNT properties through molecular mechanics is well suited to do so as the elastic modulus found is comparable to that obtained from ab-initio calculations.

3.1.1 *Importance of Area definition at nanoscale*

We already have pointed out that the area of the system on which the tensile and compressive force is applied, has a significant role to define the value of modulus. In order to emphasize the significance of the cross sectional area of carbon nanotube in the evaluation of axial modulus, we now look and compare few different cases. Before we proceed here are few useful facts:

For a nanotube of a given chirality (n, m) the diameter (in angstrom) is given by:

$$D = \frac{2.46}{\pi}\sqrt{n^2+nm+m^2}$$

The interlayer thickness for graphite layer is 3.4 A, often used as the wall thickness for carbon nanotubes or the difference between two consecutive walls in a multi-wall nanotube. This value will be referred as 't'.

The mean radius $\left(\frac{r_i+r_o}{2}\right)$ of (10, 10) nanotube is 6.78 A that is approximately equals to 2t.

Area calculation for (10,10) isolated nanotube:

For cases where the isolated nanotube is assumed as a thin shell, the area is computed as:

$$A_1 = \pi(r_i+t)^2 - \pi r_i^2 = 46.10\pi$$

Where r_i represents the inner radius of the tube.

In many works this expression has further been simplified to:

$$A_2 = \pi(r_i+t)^2 - \pi r_i^2 = 2\pi r_i t \text{(Cai, Bie et al. 2004; Chandra, Namilae et al. 2004)} = 34.54\pi$$

In the beam assumption, the area is taken to be:

$$A3 = \pi(r_i+t)^2 = 71.91\pi$$

Hence for the very definition of area, and the same value of $\frac{\partial^2 E}{\partial \varepsilon^2}$, the value of the reported modulus for identical cases can be widely different. We have here left aside the fact that there might even be disagreement in the value of thickness

of the shell itself leading to even more diversity in reported values. While our work uses interlayer spacing of graphite (3.4 A) as shell thickness of nanotube, very different values like 0.66 A (Yakobson, Brabec et al. 1996), 0.75 A (Tu and Ou-Yang 2002) are also found in literature.

3.1.2 Predicting the elastic modulus

Elastic modulus of carbon nanotube is primarily dependent on its bond and angle strengths. This is mainly due to chemical bonding interactions and these do not vary across different size and shape of carbon nanotubes. Hence, the observed drastic variations in reported values from theoretical calculation are mostly because of the use of different definitions of the cross sectional area. To further emphasize the above claim a problem was formulated on the basis of the available data of isolated (10, 10) nanotube. Based on this data an attempt was made to predict the modulus of other isolated armchair nanotubes. The only assumption in deriving such an equation is that the modulus is different solely due to different area involved. Since we know that the number of bonds and angles is linearly related to the number of atoms in an infinitely long nanotube, the force required to strain the system can be related accordingly. Hence for an isolated (n, n) armchair single-wall nanotube taking the assumptions into account we can show that for beam approximation:

$$Y_{(n,n)} = \frac{\sigma}{\varepsilon} = \frac{\frac{n}{10}F_{(10,10)}}{\varepsilon} = \frac{nF_{(10,10)}}{10\varepsilon A_{(n,n)}}$$
$$= \frac{nF_{(10,10)}}{10\varepsilon\pi(0.68n+1.7)^2}$$
$$= \frac{nF_{(10,10)}(6.8+1.7)^2}{10\varepsilon A_{(10,10)}(0.68n+1.7)^2}$$
$$= Y_{(10,10)}\frac{2.5n}{(0.4n+1)^2} \quad (11)$$

And similarly for thin shell approximation:

$$Y_{(n,n)} = \frac{\sigma}{\varepsilon} = \frac{\frac{n}{10}F_{(10,10)}}{\varepsilon} = \frac{nF_{(10,10)}}{10\varepsilon A_{(n,n)}}$$
$$= \frac{nF_{(10,10)}\left((6.8+1.7)^2-(6.8-1.7)^2\right)}{10\varepsilon A_{(10,10)}((0.68n+1.7)^2-(0.68n-1.7)^2)}$$
$$= \frac{nF_{(10,10)}(13.6)(3.4)}{10\varepsilon A_{(10,10)}(1.36n)(3.4)} = Y_{(10,10)} \quad (12)$$

Here we have taken 6.8 A to be the mean radius of a (10, 10) nanotube. Simultaneously we calculated the effect of helicity and diameter of carbon nanotube on its mechanical properties through molecular mechanics. In the following, Figure 4 clearly shows that the drastic difference in reported mechanical property values arise from the use of different area definition. The beam choice for area definition shows substantial decrease of modulus as the diameter increases. Simple extrapolation of this assumption leads to a zero value of modulus for infinite diameter, i.e. single sheet of graphene.

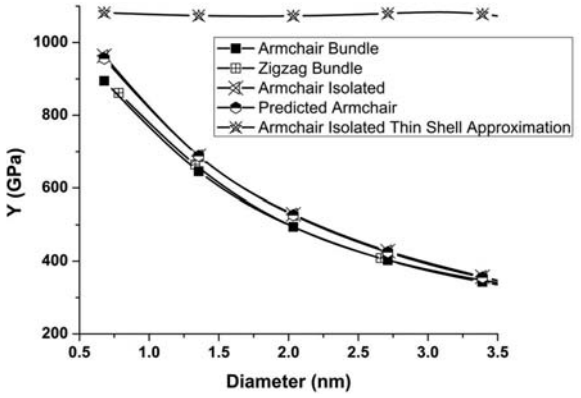

Figure 4: Axial Modulus of Single-wall Carbon Nanotube.

From inspection of Figure 4, we observe the following:

1. Elastic modulus of carbon nanotube does not depend on helicity of the tube. This is in agreement with our expectation, as we mentioned earlier that the strength of C–C bond and C–C–C angle are the primary factors in determining the modulus that does not vary

with helicity. Since the comparison is between (almost) same diameter tubes of armchair and zigzag nanotube the area factor does not make any difference here.

2. Using beam assumption of nanotube we see a decrease in elastic modules as the tube diameter increases.

3. Using a thin shell approximation of nanotube, we see that the diameter has almost no effect on elastic modulus of nanotube.

4. Another conclusion clearly follows from the points raised in #2 and #3; From the use of two different area definitions, one may conclude presence of two different trends on the influence of the diameter of nanotubes on their elastic modulus. This is misleading.

5. Finally, we observe that the predicted value from the equation 11 and 12 gives us good match with the value of elastic modulus calculated by molecular mechanics calculation backing the claim that the major difference in values is primarily due to the definitions and less likely due to the physical properties of the system itself.

3.2 Elastic Modulus of Multi-wall nanotubes

Similar to the calculations of single-wall nanotubes, we carried out molecular mechanics calculations to find the young's modulus of multi-wall nanotubes bundles. We observed that the multi-wall nanotubes have a greater young's modulus than the single-wall nanotubes as found in literature (Sanchez-Portal, Artacho et al. 1999). We carried out these calculations on multi-wall nanotubes with different radii (inner and outermost) and different chirality. To assess the asymptotic behavior, we have also calculated the elastic modulus of graphene structures with different number of layers, i.e. the limiting case is graphite.

We also attempt to find the Young modulus for an isolated multi-wall carbon nanotube assuming a beam with layers (10, 10), (15, 15) and so forth. This is similar to the derivation of equation 11 for the Young modulus expression with a beam approximation for an isolated single-wall carbon nanotube. If total 'm' layers are assumed in MWNT, with the innermost being (10, 10), we can express the total force on the MWNT as the summation of all the forces on each tube. In order to calculate the cross sectional area needed to find the Young's modulus we consider the outer most tube in the 'm' layers. Accordingly we can write,

$$Y_{MWNT_{ISOLATED}}\varepsilon = \sigma = \frac{F_T}{A} = \frac{Fm(2+(m-1)0.5)}{2\pi(1.7)^2(2(1+m)+1)^2} \tag{13}$$

$$\Rightarrow Y_{MWNT_{ISOLATED}} = \frac{6.25m(m+3)}{(2m+3)^2} Y_{(10,10)_{ISOLATED}} \tag{14}$$

This simple formula does not take into account the inter layer van der Waals attraction and possible effect of the radius of curvature of different walls. However it does a good job in predicting the modulus values as evident from Figure 5. From equation 14 given above, we also find that as $m \to \infty$ the value of the modulus of a multi-wall nanotube with (10, 10) tube being the innermost tube approaches a constant value:

$$Y_{MWNT_{ISOLATED}} = \frac{6.25}{4} Y_{(10,10)_{\text{ISOLATED, Beam Approximation}}}$$
$$\sim 1TPa, \text{ using a value } \sim 640GPa \text{ for } Y_{(10,10)}$$

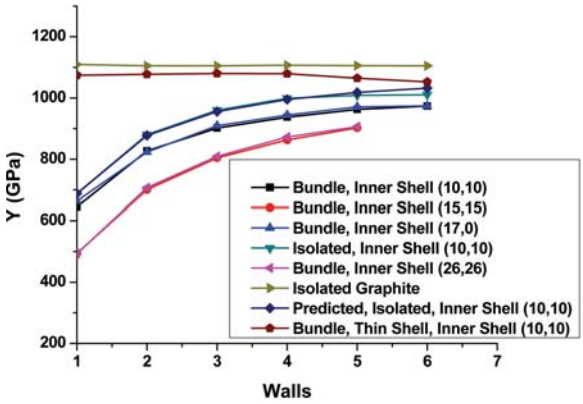

Figure 5: Axial elastic modulus of various multi-wall carbon nanotube.

From Figure 5, the observed points are listed as following:

1. We observe that with increased number of walls the modulus of the nanotube increases and finally approaches close to $\sim$ 1 TPa.
2. Thin shell approximation yields a value of $\sim$ 1 TPa independent of the number of tubes.
3. The predicted value for the isolated multi-wall nanotubes matches well with calculations from molecular mechanics method proving the validity of our assumption.
4. From #3 observation we also conclude that the van der Waals interaction among the tubes does not contribute much to the modulus as our prediction did a good job without taking that factor into account.
5. For isolated graphite sheets the modulus value does not change with increasing number of layers, in agreement with our conclusion in #4.

Structure of Multi-wall nanotube: We observed another interesting fact from the molecular mechanics study of carbon nanotube. We find that the minimized structure of the multi-wall nanotube in a bundle does not remain circular anymore agreeing with experimental observations (Ruoff, Tersoff et al. 1993). For more number of walls the outer walls tend to take a shape of hexagon. Figure 6 shows the hexagonal shape for a tube made from (15, 15), (20, 20), (25, 25), (30, 30) and (35, 35) tubes. The transition from circular to hexagonal shape, while moving from inner to outer walls, is clearly observed here.

This evolving hexagonal outer structure leads to a more efficient packing of bundles of thicker MWNT. Since nanotubes are widely used and anticipated as one the most favorable candidates as nanofillers in nanocomposites, this definitely is an interesting finding. It may result in very different surface and interface properties in nanocomposite made from multi-wall nanotube with respect to those made from single-wall nanotubes. The tendency of the outer wall tubes to form a hexagonal structure is clearly due to a delicate balance between the van der Waals forces acting between the walls and strain energy induced due to curvature. This tendency is the same tendency seen in large diameter single-wall carbon nanotube which form a collapsed stable structure as shown earlier by one of us (Gao, Cagin et al. 1998).

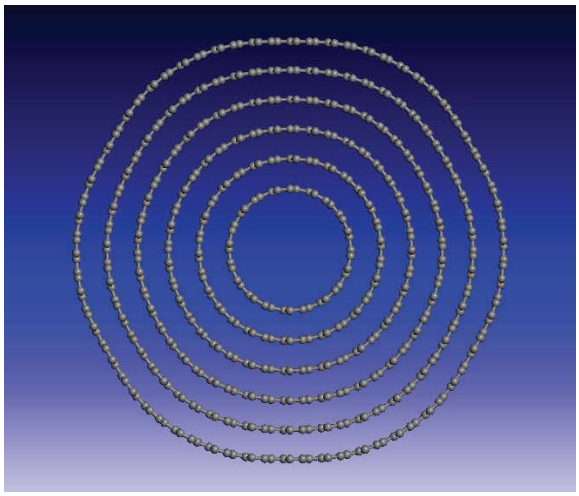

Figure 6: Optimized structures of a MWNT looking down cylinder axis. The hexagonal shape evolves so as to minimize the strain energy due to curvature by enhancing layer-layer van der Waals interactions. Force fields without van der Waals interactions may miss this shape change.

3.3 Twist/Torsion modulus of Carbon Nanotubes

Torsion modulus or twist modulus is another important property in assessing mechanical strength of a nanotube. In reality, the nanotube is more likely to be in a twisted form than otherwise. Torsion modulus was calculated for isolated carbon nanotube assuming it to be a thin wall hollow shaft. The strain energy in torsion in that case is given by:

$$U = \frac{GJ\theta^2}{2L} \tag{15}$$

Where

$J = 2\pi r^3 t$
U= Strain Energy
G= Torsion modulus
θ = Twist Angle in radian
r = mean radius of the shaft wall
t = thickness of the tube
L = Length of the tube

We will use two approaches in determining the twist modulus: tubes with finite length and infinite length (through the use of periodic boundary conditions in axial direction).

3.3.1 Single-wall nanotubes

Finite length: Non-periodic system of nanotube was built. Keeping one end fixed the other end was strained in terms of twist in an increment of 2°. The twist was applied both in clockwise and anticlockwise direction. We fitted the strained energy calculated and different amount of twist to equation 15. This gave us the twist modulus for nanotubes. Figure 7 gives a comparison of the modulus obtained of (almost) same diameter of zigzag and armchair nanotubes of different lengths.

Conclusions drawn from the observation of figure 7 are:

1. The twist modulus decreases with increasing length of the tube as expected.
2. Zigzag nanotubes shows a higher twist modulus than armchair nanotubes agreeing with the available literature findings (Wang, Wang et al. 2004; Alford, Landis et al. 2005)
3. As the length of the tube is increased the modulus tends to take an asymptotic nature and tries to converge to a value in both types of nanotubes.
4. The difference between the modulus of two types of nanotubes with the same diameter decreases as the length of the tubes increase.

We further examined the dependence of modulus on the diameter of the tube. Figure 8 and 9 show the diameter dependence of the torsion modulus of different lengths of nanotubes (armchair and zigzag).

We observe contrary to (Wang, Wang et al. 2004) and in agreement with (Popov, Van Doren et al. 2000; Alford, Landis et al. 2005) that the diameter has hardly any effect on torsion modulus.

Infinite single-wall nanotube:

We extended our study to investigate the twist modulus of an infinite isolated nanotube through the novel use of periodic boundary conditions imposed in z-direction. In a periodic model, due to presence of periodic image atoms the application of twist is entirely different than how its finite length counter part was dealt. The whole process of twisting an infinite isolated nanotube (m, m) and finding the torsion modulus from it consisted of the following steps:

1. Build the model
2. Select atoms on one boundary of the cell in z direction.
3. Rotate the selected atoms by $\frac{2\pi}{m}n$ (only discrete rotations, based on m)
4. Fix the rotated atoms and also fix the atoms on the other boundary of the unit cell
5. Maintaining the above constraints relaxed the structure through minimization by ab initio calculations based force fields.
6. Recalculate the bonds at the boundaries and reformed to give the desired twist to the nanotube structure.
7. A final minimization of the structure with all moveable atoms.

The final twisted nanotube, built on the above procedure is pictured in figure 10 when viewed from front and looked into the z direction.

Figure 11 shows the potential energy profile obtained for a 49.2 nm long twisted tube as a contour plot. The procedure described above was repeated for different values of 'n' and figure 12 was obtained while plotting the energy of the strained tube with twist angle. The straight line obtained was fitted to equation 15 to evaluate the twist modulus of the tube. Figure 12 shows the energy vs. torsional-strain variation obtained from the calculation.

Calculation of torsion modulus in this method is then carried out for different armchair and zigzag SWNT's with different set of c-axis values ('z' direction). The results obtained are summarized in Table 2. The modulus found agrees reasonably with the values reported in literature (Lu 1997;

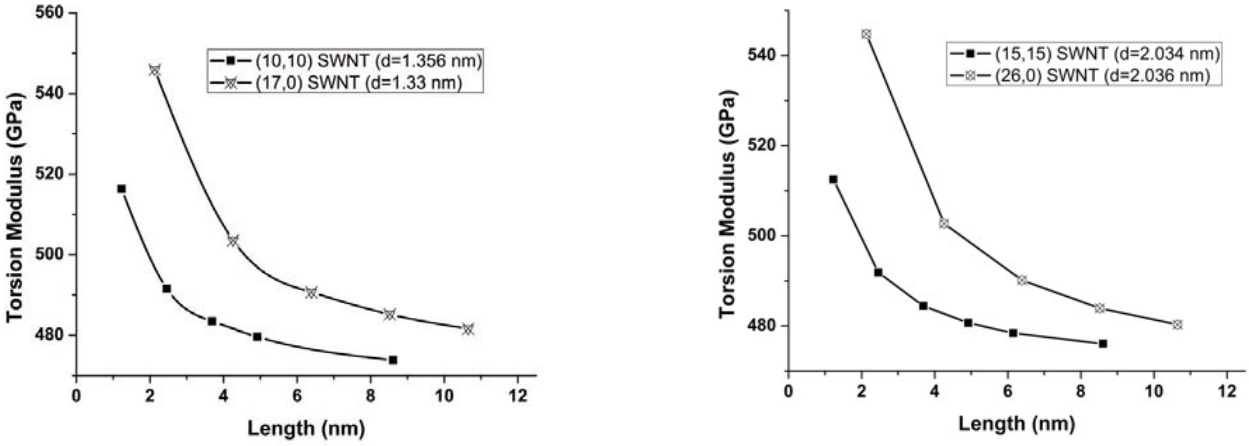

Figure 7: Variation of twist modulus for zigzag and armchair CNTs for two different diameters (a) d=1.35 nm, (b) d=2.04 nm as a function of finite length of the tubes.

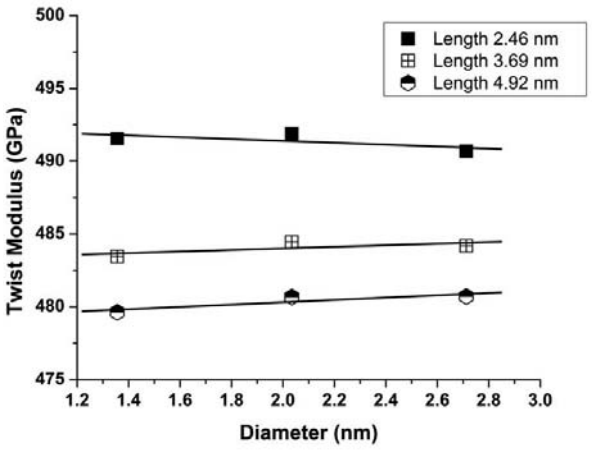

Figure 8: Twist modulus (Armchair)

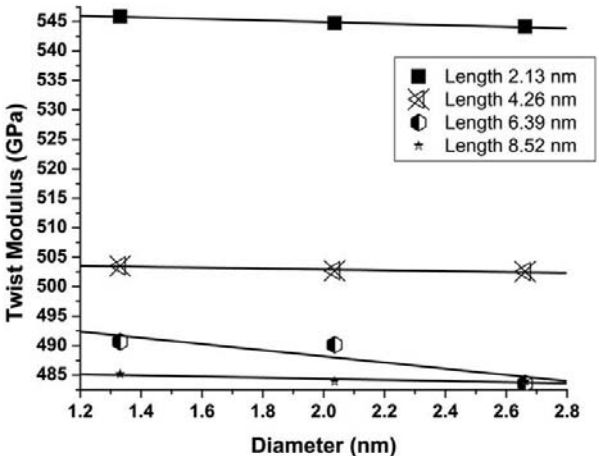

Figure 9: Twist modulus (Zigzag)

Table 2: Torsion Modulus of infinite single-wall nanotube.

SWNT	Torsion Modulus (GPa)	Length of periodic cell (nm)
(5,5)	452.85	49.2
(5,5)	462.33	98.4
(10,10)	463.48	24.6
(10,10)	466.77	49.2
(15,15)	465.10	24.6
(15,15)	437.8	73.8
(10,0)	464.83	42.61
(15,0)	462.47	42.61
(20,0)	460.46	42.61

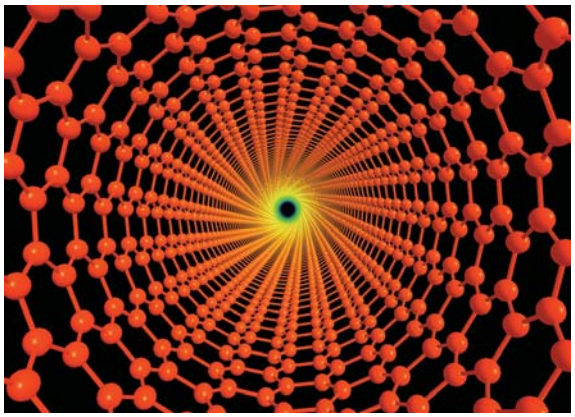

Figure 10: Axial and lateral views of a twisted carbon nanotube.

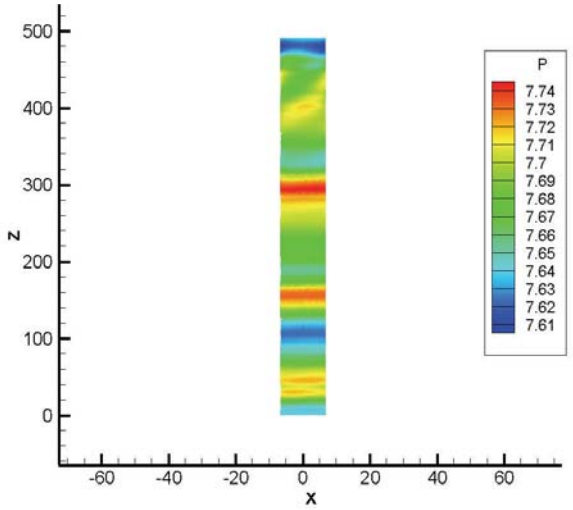

Figure 11: Potential Energy (kcal/mol) content contour plot for a twisted nanotube determined for a configuration from molecular dynamics at T=300 K. The length of tube is 49.2 nm.

Alford, Landis et al. 2005; Xiao, Gama et al. 2005).

Conclusions made from observation of Table 2 are listed as following:

1. As expected from the observations of the twist modulus study of finite length nanotube, the torsion modulus of an infinite long nanotube converges to a value irrespective of the chirality and diameter of the tube.

2. The claim of higher twist modulus of zigzag nanotube with respect to armchair nanotube, based on finite limit calculations is not valid in the infinite limit as twist modulus of both armchair and zigzag nanotube converges to same value

3. The converged value of the twist modulus for both type of nanotube is roughly 460 GPa.

3.3.2 Twist Modulus of Multi-wall carbon nanotube

Finite length:

Keeping in mind that nanotubes used for practical purposes are of high aspect ratio, infinite length calculation results are more important than the finite ones. However due to the approach implemented above, not too many calculations are possible for multi-wall nanotube. Rotation by same angles of more than one tube and rearrangements of bonds at the same time at the boundary leaves us with very few choices. From the observations made for single-wall nanotube behavior with ap-

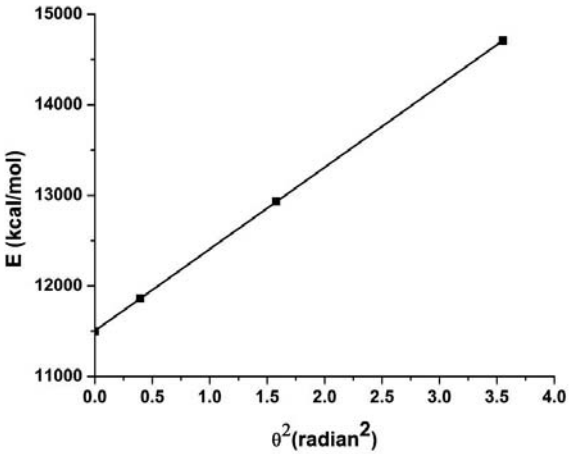

Figure 12: Variation of Energy with respect to twist angle for (10, 10) CNT.

plied torque, the lengths of the multi-wall nanotube considered were higher. Higher length finite length nanotube gave results close to infinite ones. Table 3 summarizes the results obtained. The notation n_m_p MWNT stands for a MWNT with inner tube (n, n) and the outer tube (m, m) and the cell length in z-axis is p times the unit cell length (2.46 nm). It is important mentioning here that we assumed a no slip condition between the tubes. All the tubes in a multi-wall nanotube are rotated by the same angle when a torque is applied.

A quick comparison of these few data tells us that

1. Adding another wall does not affect the twist modulus and the values are close to those of infinite length single-wall nanotube twist modulus.

2. We observe no dependence of diameter and number of walls on the twist modulus. It is expected that this value should also be similar to graphite sheet shear modulus, as tubes with very big diameter and large number of walls can be approximated as layer of graphite sheet. To verify, elastic constants of graphite sheet were also evaluated by the same force field and the shear modulus was found to be 457.63 GPa, comparable to the values obtained above.

3.4 Structure, Mechanics and Stability of Carbon Nanotori

To understand the energetic related to nanotube bending we looked into nanotori structures made of carbon. Nanotorus is a nanotube bended into a ring. We constructed nanotori and studied its strain energies, which gave us a measure of the bending stiffness of a nanotube. One of the earliest computations on this property was conducted and presented at Foresight conference by Caltech group (Gao, Cagin, Goddard) in nineties.

Armchair carbon nanotube of different length and radius was made into a circular tube. The structure obtained was then minimized and the strain energies of the tubes were determined. Below, we have given a configuration obtained through minimization of a (10, 10) nano-torus with a mean radius = $\frac{49.2nm}{2\pi} = 7.83nm$. We observe the emergence of kinks in the minimized structure. While tension prevails in the outer wall, the inner wall remains in compression. This leads to development of kinks in the inner wall to localize the strain energy. We will later show that heating of nanotori sometimes can help in annealing kinks to homogenize the location and number of kinks. Thermal annealing distributes the kinks more evenly throughout the structure and helps get the structure out of local minima to an energetically more favorable structure. One such kink is zoomed from the above-obtained structure and given below in figure 14.

As seen in figure 14 the circular cross section becomes more oval sized due to brazier effect (Falvo, Clary et al. 1997). The narrowest cross section approaches close to the inter layer spacing of graphite which is 3.4 A. As observed in figure 15, those are the regions with high energies. Kinked carbon nanotubes has also been studied using bond-order potential energy function and self-consistent tight-binding scheme (Brenner, Shenderova et al. 2002).

Table 5 gives the strain energies of different nanotori calculated using the energy of infinite-straight nanotube as reference. Hence the energies correspond to strain energy is due to bending only. We observe from the strain energies obtained, that

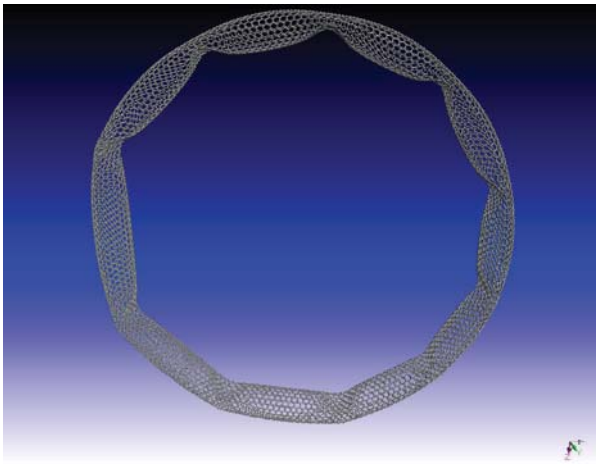

Figure 13: Nanotori of (10, 10) nanotube.

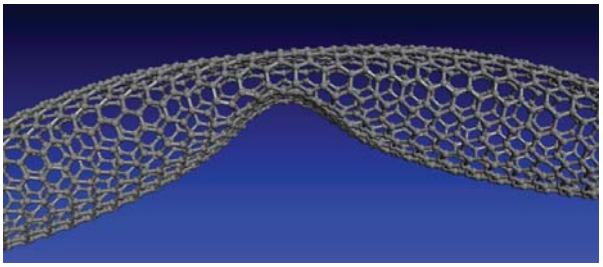

Figure 14: Kink in Nanotori.

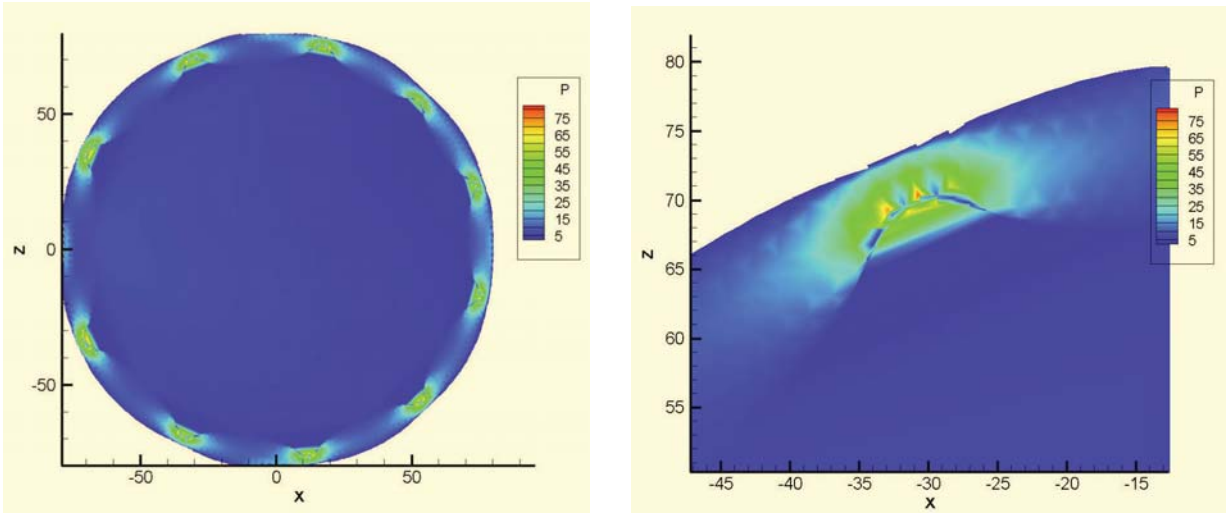

Figure 15: Contour of Potential Energy (kcal/mol) of SWNT (10, 10) Nanotori.

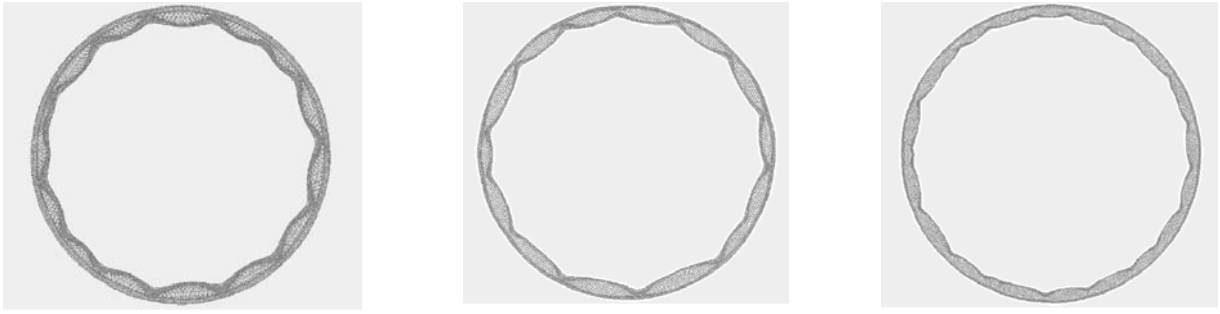

Figure 16: Smoother structure of (15, 15) nanotori with radius from left R=7.83 nm, 11.745 nm and 15.66nm.

Table 3: Twist modulus of finite length MWNT.

MWNT	Length of the tube (nm)	Torsional Modulus (GPa)
10_15_25	6.15	471.77
10_15_50	12.3	469.03
15_20_25	6.15	472.58
15_20_50	12.3	469.51
10_15_20_25	6.15	472.45
10_15_20_50	12.3	469.52

Table 4: Strain Energy of Single-wall nanotori.

Nanotube	Mean radius of Nanotori (nm)	Energy/atom (Kcal/mol)	Strain Energy (ΔE) (Kcal/mol)
(10,10)	1.9576	8.1676	5.291
(10,10)	3.9152	5.4987	2.6220
(10,10)	7.83	4.1936	1.3169
(10,10)	11.745	3.8910	1.0143
(10,10)	15.66	3.5031	0.6264
(10,10)	23.49	3.1873	0.3106
(10,10)	31.32	3.063	0.1863
(10,10)	39.15	3.0087	0.1319
(10,10)	Infinite	2.8767	0
(15,15)	7.83	3.5204	1.3034
(15,15)	11.745	3.182	0.9649
(15,15)	15.66	3.021	0.8039
(15,15)	23.49	2.7699	0.5528
(15,15)	Infinite	2.2171	0
(20,20)	7.83	3.0076	1.0275
(20,20)	11.745	2.818	0.8379
(20,20)	15.66	2.7451	0.765
(20,20)	Infinite	1.98	0

longer tube and hence nanotori with larger radius are more easily formed than the shorter ones as expected. Similarly we observe that nanotubes with bigger diameter are easier to bend into nanotori than their shorter diameter counterpart of same length. Given in figure 16 are the minimized structures of (15, 15) SWNT nanotori. Diminishing number of kinks are observed as we move from lower to higher radius nanotori as expected due to reduction in strain energy.

Figure 17 shows an exponential decay of strain energy with increasing radius of the nanotori. We see that after a certain radius, around 20 nm the curve becomes asymptotic and we expect that it is around this point onwards the appearance of kinks are almost negligible. This observation goes well with the findings in (Cagin, Gao et al. 2006) where it was found that for (10, 10) nanotori with radius more than 18.83 nm the stable structure is smooth nanotori. Fitting with an exponential function yielded the following relationship:

$$E = 7.66\exp(-r/4.52) \tag{16}$$

where E and r are in Kcal/mol-atom and nm respectively. From equation 16, we find that the rate of change of strain energy per atom becomes negligible (less than 0.026 Kcal/mol–atom) when the torus radius becomes greater than 18.83 nm. This radius is the limiting value above which the stable structure of the nanotori becomes kink-free

and smooth. However the present study does not look into the possibility of having both stable and kinked structure of nanotori that has a radius between 10.03 and 18.83 nm as pointed out in the same work.

Figure 17 when redrawn in a different manner as in figure 18, i.e. with respect to curvature, the slope of the linear fit obtained, is then a measure of the bending modulus of a nanotube. In this manner, we have obtained the bending modulus for (10, 10) nanotube as 305 GPa. The initial points from the above figure were discarded as the strain energy obtained at such small radii is also influenced by the presence of kinks other and hence will lead improper values for bending modulus of nanotubes.

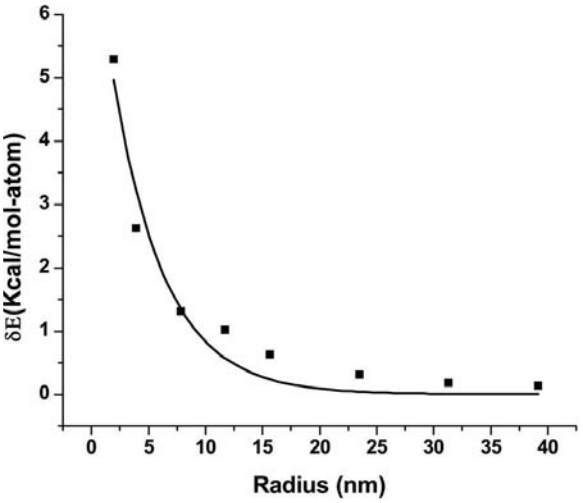

Figure 17: Variation of strain energy with radius of (10, 10) nanotori.

In other works on nanotori, Huhtala et. al (Huhtala, Kuronen et al. 2002; Huhtala, Kuronen et al. 2002) looked into minimum energy structure and thermal stability of large nanotori structures using Brenner potential using molecular dynamics simulation. Potential energy of the structures was monitored to determine the relation between the critical buckling diameters with that of the nanotori diameter. The strain energy of the tubes per atom basis was found to be linearly related (increasing) when the tube diameter is approximately less than that of a (10,10) tube. Cagin et

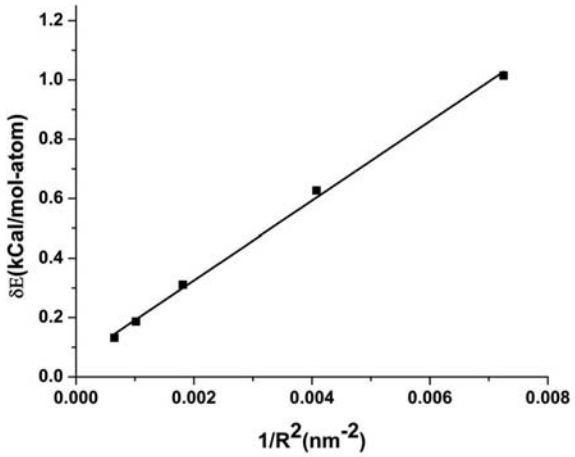

Figure 18: Strain Energy of Nanotori proportional to inverse of radius squared.

al (Cagin, Gao et al. 2006) have also looked into the problem of determining the critical diameter for smooth single-wall nanotorus and the bending modulus. They found that nanotori could exhibit more than one stable structure within the thermal fluctuations, which are thermally equivalent.

Multi-wall nanotube nanotori:

With mean nanotori diameter (7.83 nm), a triple wall nanotori from (10, 10), (15, 15) and (20, 20) nanotubes and two double-wall nanotori from (10, 10), (15, 15) and (15, 15), (20, 20) nanotubes were constructed. Optimization of their energy and structures using molecular mechanics methods gave us figure 19. We observe that the kinks in these structures emerge almost in parallel to each other on each wall. Table 5 gives the values of the strain energies obtained for the double wall nanotori made from (10, 10) and (15, 15) nanotubes.

The strain energies of multi-wall nanotori were found to be higher than those of single-wall nanotori. This is expected, as the presence of inter wall van der Waals forces restricts the freedom of all the atoms on different walls to move and shift into a less-strained configuration. The potential energy contour plot (Figure 21) shows that the inner tube has higher energy which is expected due to the constraint put by the outer wall on its movement.

Figure 20 shows that adding more walls increase

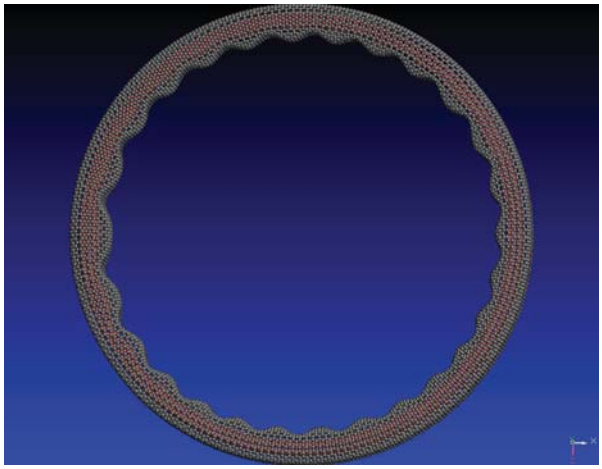

Figure 19: MWNT nanotori.

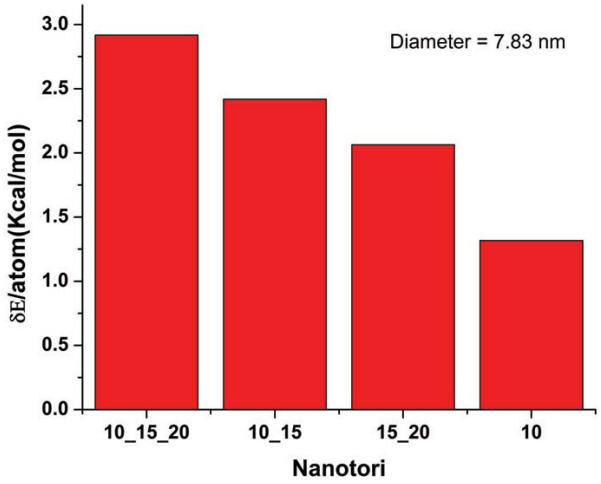

Figure 20: Strain energy of MWNT nanotori.

Table 5: Strain Energy of multi-wall nanotube.

Radius (nm)	Energy per atom (Kcal/mol)	Strain Energy per atom (Kcal/mol)
7.83	4.01	2.42
11.745	3.15	1.55
15.66	2.89	1.29
Infinite	1.60	0.0

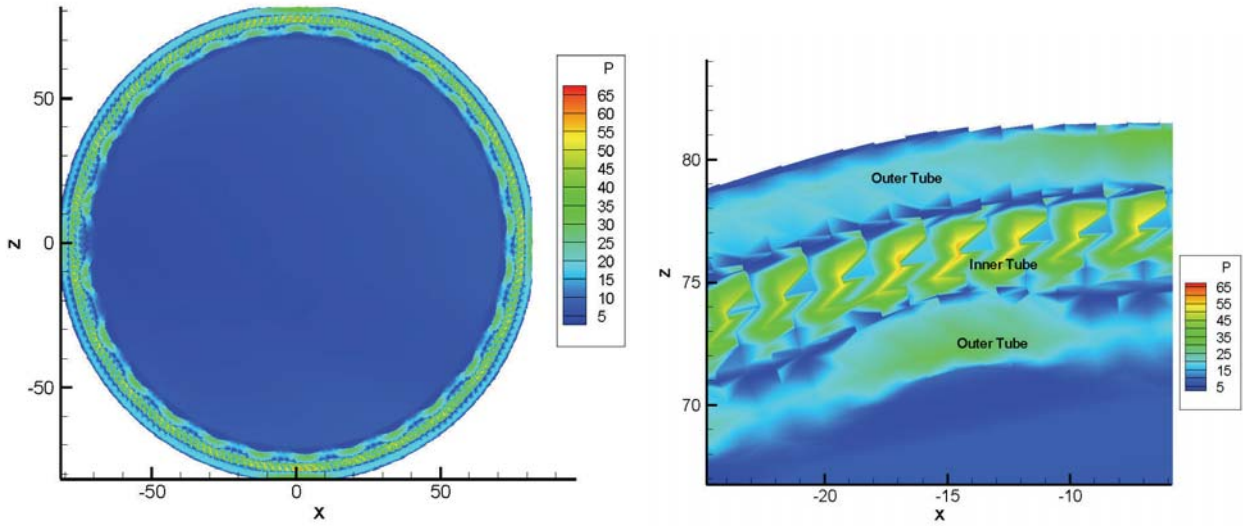

Figure 21: Potential Energy Contour in a MWNT Nanotori.

the strain energy of nanotori. However for same number of walls, it seems that larger the outer tube diameter, lesser will the strain energy be. This is along the same lines with the result obtained for nanotori of a single-wall nanotube.

Twisted Nanotori:

Liu et al. (Liu, Zhang et al. 2005; Liu, Zhang et al. 2005) performed atomistic simulations of defect free single and multi-wall nanotori. In their studies, they have concluded that torsion helps to reduce the strain energy of single-wall nanotori; in contrast it tends to destabilize multi-wall nanotori. The magnitudes of twists applied to the

tubes were multiples of 2π. These values, given the mean torus radius, are somehow larger than usual. In the present work, we also have looked into the behavior of twisted nanotori. The twist in this case was given in small increments, integer multiples of $\frac{\pi}{10}$ (least possible unit value dictated by (10,10)-tube) as opposed to the above study. Nanotori made of (10, 10) SWNT was constructed with a nanotori diameter of 46.98 nm. Twists of different angles were given to the structure (by rearrangements of bonds as torus constructed by identifying ends). Table 6 gives the values of the strain energies obtained.

Since the above table is based on single nanotori, the effect of bending is same in all the cases. Hence, we expect that the strain energy would be directly proportional to the square of the angle by which it was twisted. This is clearly observed in Figure 22.

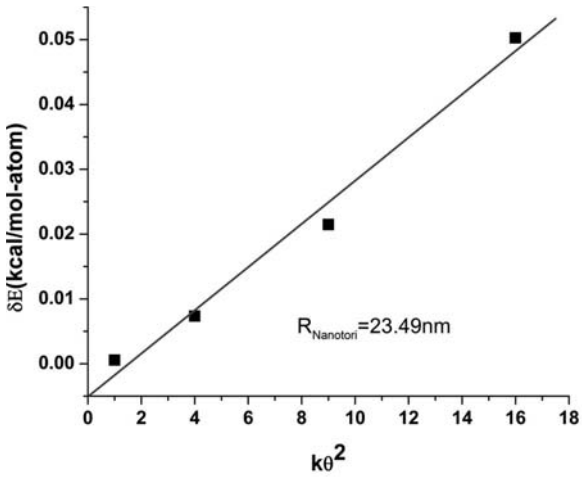

Figure 22: Strain energy of a twisted (10, 10) nanotori for same radius and different angles.

4 Thermal Properties of Nanotubes

4.1 *Effect of Temperature on axial modulus of Single-wall nanotube*

All molecular mechanics and density functional level of theory results in this work do not take into account the effect of temperature. However in reality it is of utmost importance to know the influence of temperature, as very rarely an application would be used at very low temperatures. Temperature effect on stress-strain behavior, and resulting axial modulus of (10, 10) nanotube was studied using molecular dynamics. Simulations were carried out from T=100 K to T=700 K in increments of 100 K. At each temperature a zero stress simulation was followed by simulations at 2, 4 6, and 8 GPa, tensile and compressive stresses along c-axis. The constant temperature constant stress (NPT) MD simulation data is collected over 400 picoseconds for calculating the resulting compressive and tensile strain to determine the elastic modulus. The result for axial modulus vs. temperature is plotted in Figure 23. We observe almost a linear thermal softening effect in the studied temperature range, approximately with a slope of 26 MPa/K.

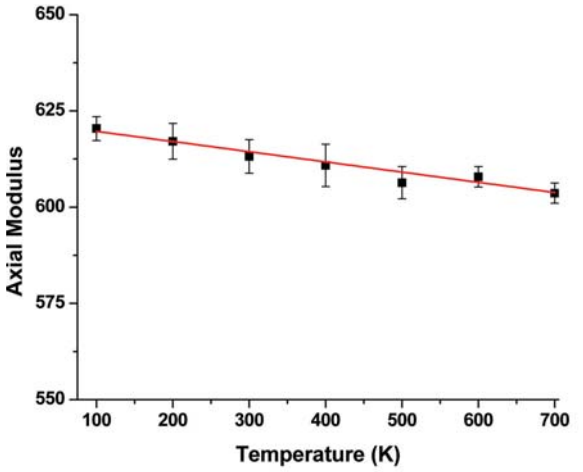

Figure 23: Effect of temperature on axial elastic modulus.

As we have observed earlier that elastic modulus in axial direction for nanotube does not depend on the chirality, similar temperature dependence can be expected for nanotubes of other chirality. The temperature coefficient of elastic modulus 26 MPa/K implies a 2.6 GPa decrease over a 100K operation range (around 0.3% of the value), which is considerably small. Hence for all practical purposes one can safely assume the elastic modulus of nanotube as constant in presence of other more sensitive parameters, alignment, defects, impurities, etc.

Table 6: Strain Energy of twisted nanotori.

Nanotube	Radius (nm)	θ (Degrees)	Energy per atom (kcal/mol)	Strain Energy per atom (Bending plus torsion) (kcal/mol)	Strain Energy per atom (Torsion) (kcal/mol)
(10, 10)	23.49	0	3.1873	0.3106	0
(10, 10)	23.49	36	3.1878	0.3111	0.0005
(10, 10)	23.49	72	3.1946	0.3179	0.0073
(10, 10)	23.49	108	3.2088	0.3320	0.0215
(10, 10)	23.49	144	3.2376	0.3608	0.0503

4.2 Thermal expansion of nanotubes and nanotube bundles

Carbon nanotubes are deemed to show negligible expansion on heating. To validate this assessment, we have chosen a (10, 10) carbon nanotube bundle consisting 1600 atoms and performed molecular dynamics simulation under atmospheric pressure conditions at temperatures starting $T = 100K$ to $T = 700K$ with increments of $100K$. Figure 24 shows the thermal expansion in axial direction. It is obvious that there is negligible expansion over 600 K range. The linear thermal expansion coefficient for (10, 10) tube, assuming constant thermal expansion was calculated to be: $\alpha = \frac{1}{L}\left(\frac{\partial L}{\partial T}\right)_P = 1.24 \times 10^{-6}/K$ agreeing reasonably with literature (Maniwa, Fujiwara et al. 2001; Li and Chou 2005).

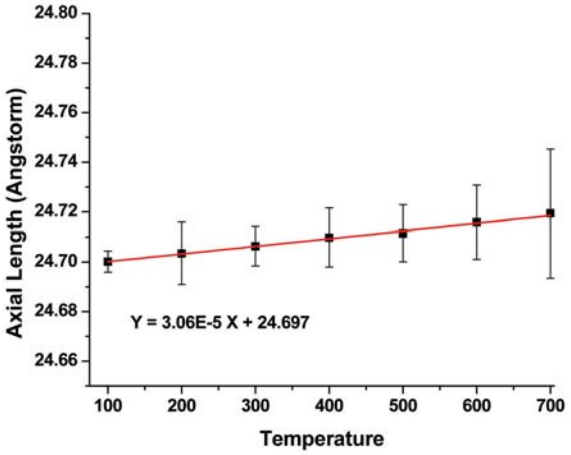

Figure 24: Thermal expansion of nanotube in axial direction.

We determined the variation of density, volumetric thermal expansion and linear expansion in a- or b- axis directions. The off axis thermal coefficient expansion obtained from the relation $\beta_r = \frac{\gamma_v - \alpha}{2}$ where γ_v is volume expansion coefficient and α is axial expansion coefficient, was $9.6 \times 10^{-6}/K$. This is larger than axial linear expansion by a factor more than 7. This is understandable since it is essentially a result of the increased anharmonicity in tube-tube van der Waals interactions.

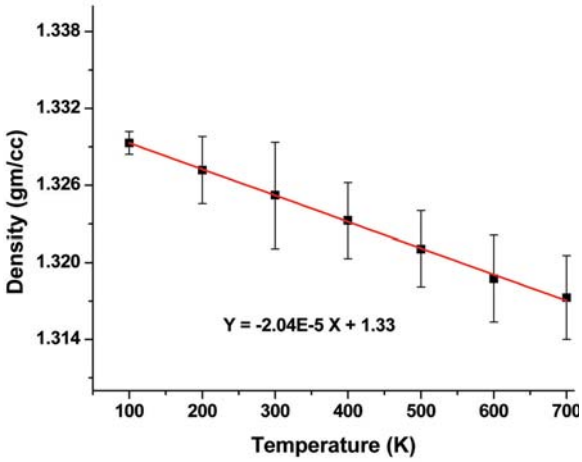

Figure 25: Density variation of SWNT bundle with temperature.

4.3 Kinks in Nanotori as Local Strain Energy Sinks/Sources

Disappearance of kinks upon heating:

To study the rich configurations that result due to presence of kinks as in Cagin et al (Cagin, Gao et al. 2006), we have performed molecular dynamics simulations on a nanotori of (10, 10) nanotube with a mean radius of 7.83 nm. We per-

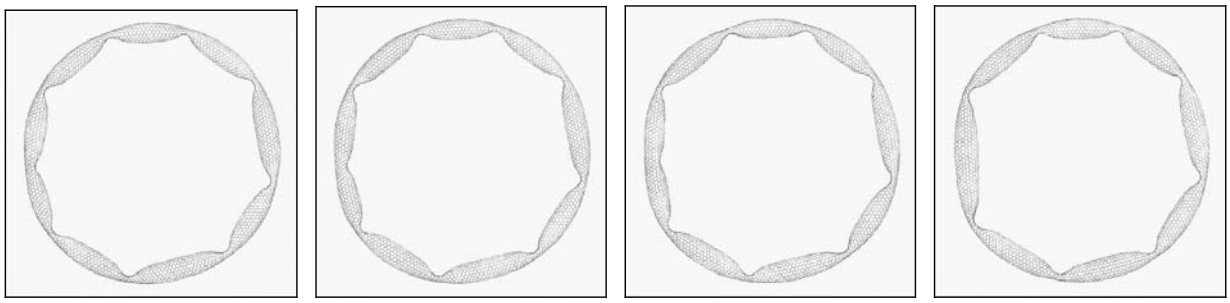

(a) **(b)** **(c)** **(d)**

Figure 26

formed a 50-ps constant temperature simulation at T=300 K. We observe that the structure resides in a metastable state with higher number of kinks. Thermal fluctuations help overcoming the barriers between N and N-1 kink structures after around 40-45 ps. The sequence in Figure 26 demonstrates this process.

We observe that a kink on the middle left portion of the ring as gradually disappeared from figure 26(a) to figure 26(d) as indicated. The time variation of the potential energy in Figure 27 apparently shows the energy drop pointing the annealing of one of the kink-defects.

The time span involved in such drop is also quite large, so the structure remains in one of the N-kink meta-stable state for almost 40 ps. We have calculated the amount of potential energy associated with this transition is $\sim$ 200 kcal/mol. The model structure studied contains 8000 atoms. Hence, the corresponding change in potential energy per mol atoms only, $\frac{300\times1000}{8000} = 37.5$cal. If we compare this with the mean kinetic energy content of an atom at 300K, RT $\sim$600 cal/mol. Clearly, the barrier height per atom mol is within the variance of kinetic energy per atom at room temperature. Hence, we show that thermal fluctuations are strong enough to help the structure get out of metastable states local minima and move to a favorable structure with fewer kinks.

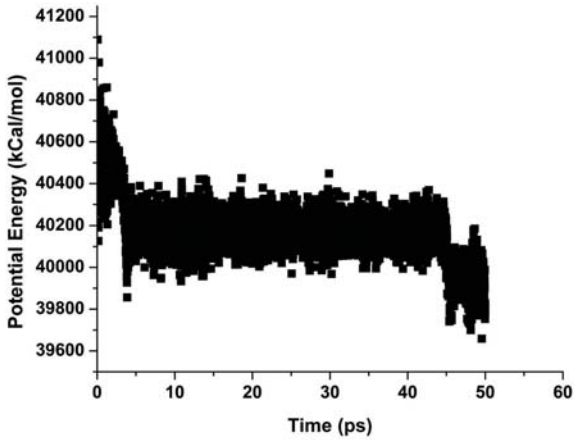

Figure 27: Potential energy profile during kink disappearance.

5 Concluding Remarks

We have evaluated mechanical and thermal properties of carbon nanotube and nanotori in the present work to gain insight of structure property relationship of nanotube. We observed that the definition of area used for Young's modulus calculation of nanotube is non-trivial and can be the source of difference by a significant factor. It might also be responsible for the different trends reported in literature. On this basis, we have come up with equations that address discrepancies both in values and trends of axial modulus. We also find that the van der Waals forces have the least significance in the strength of multi-wall nanotube but it can govern the structure of the outer shells. This results in a hexagonal structure with higher packing efficiency and hence, a denser system. By applying torsion to an infinite length nanotube in a novel way, we find that the claim of higher twist modulus of zigzag nanotube relative to its arm-chair counter part in the infinite limit is not valid. The effect of temperature on nanotube mechan-

ical properties was found to be minimal and for design of nanotube-based materials the temperature effect on its intrinsic properties can be neglected if the operational range is a few hundred degrees. Importance of micromechanics modeling at interface of composites is well known (S. Tchouikov, Nishioka et al. 2005). Similarly the insights gained in this study can be incorporated in designing composite materials made from nanotube. Since all the nanotube structure used were defect free in this study, we expect these results to be the ideal ones and expect some deviations in reality, due to more pronounced effects of topological defects, impurities, and alignment defects in bundles (Che, Cagin et al. 2000; Nasdala, Ernst et al. 2005; Chakrabarty and Cagin 2007).

References

Alford, J. T.; Landis, B. A. et al. (2005): Theoretical elastic properties of single-walled carbon nanotubes. *International Journal of Quantum Chemistry* **105**(6): 767-771.

Ashrafi, B.; Hubert, P. (2006): Modeling the elastic properties of carbon nanotube array/polymer composites. *Composites Science and Technology* **66**(3-4): 387-396.

Berber, S.; Kwon, Y. K. et al. (2000): Unusually high thermal conductivity of carbon nanotubes. *Physical Review Letters* **84**(20): 4613-4616.

Brenner, D. W.; Shenderova, O. A. et al. (2002): Atomic modeling of carbon-based nanostructures as a tool for developing new materials and technologies. *CMES: Computer Modeling in Engineering & Sciences* **3**(5): 643-673.

Cagin, T.; Gao, G. et al. (2006): Computational Studies on Mechanical Properties of Carbon Nanotori. *Turkish Journal of Physics* **30**: 221-229.

Cai, J.; Bie, R. F. et al. (2004): Application of the tight-binding method to the elastic modulus of C60 and carbon nanotube. *Physica B-Condensed Matter* **344**(1-4): 99-102.

Chakrabarty, A.; Cagin, T. (2007): Unpublished. *Unpublished*.

Chandra, N.; Namilae, S. et al. (2004): Local elastic properties of carbon nanotubes in the presence of Stone-Wales defects. *Physical Review B* **69**(9).

Chang, T. C.; Gao, H. J. (2003): Size-dependent elastic properties of a single-walled carbon nanotube via a molecular mechanics model. *Journal of the Mechanics and Physics of Solids* **51**(6): 1059-1074.

Che, J. W.; Cagin, T. et al. (2000): Thermal conductivity of carbon nanotubes. *Nanotechnology* **11**(2): 65-69.

Cornwell, C. F.; Wille, L. T. (1997): Elastic properties of single-walled carbon nanotubes in compression. *Solid State Communications* **101**(8): 555 - 558.

Dong, Q.; Gregory, J. W. et al. (2002): Mechanics of carbon nanotubes. *Applied Mechanics Reviews* **55**(6): 495-533.

Dresselhaus, M. S.; Dresselhaus, G. et al., Eds. (2001): *Topics in Applied Physics*. Carbon Nanotubes:Synthesis,structure,properties and application, Springer-Verlag GmbH.

Dresselhaus, M. S.; Dresselhaus, G. et al. (2004): Unusual properties and structure of carbonnanotubes. *Annual Review of Materials Research* **34**: 247-278.

Enomoto, K.; Kitakata, S. et al. (2006): Measurement of Young's modulus of carbon nanotubes by nanoprobe manipulation in a transmission electron microscope. *Applied Physics Letters* **88**(15):

Falvo, M. R.; Clary, G. et al. (1998): Nanomanipulation experiments exploring frictional and mechanical properties of carbon nanotubes. *Microscopy and Microanalysis* **4**(5): 504-512.

Falvo, M. R.; Clary, G. J. et al. (1997): Bending and buckling of carbon nanotubes under large strain. *Nature* **389**(6651): 582-584.

Gao, G.; Cagin, T. et al. (1998): Energetics, structure, mechanical and vibrational properties of single-walled carbon nanotubes. *Nanotechnology* **9**: 184 - 191.

Hohenberg, P.; Kohn, W. (1964): Inhomogeneous Electron Gas. *Phys. Rev.* **136**(3B): 864A.

Huhtala, M.; Kuronen, A. et al. (2002): Carbon nanotube structures: molecular dynamics simula-

tion at realistic limit. *Computer Physics Communications* **146**(1): 30-37.

Huhtala, M.; Kuronen, A. et al. (2002): Computational studies of carbon nanotube structures. *Computer Physics Communications* **147**(1-2): 91-96.

Klemens, P. (2001): *Theory of heat conduction in carbon nanotubes.* Proceedings of 26th International Thermal Conductivity Conference, Cambridge, MA.

Kohn, W.; Sham, L. J. (1965): Self-Consistent Equations Including Exchange And Correlation Effects. *Phys. Rev.* **140**(4A): 1133B.

Kresse, G.; Joubert, J. (1999): *Phys. Rev. B* **59**: 1758.

Krishnan, A.; Dujardin, E. et al. (1998): Young's modulus of single-walled nanotubes. *Physical Review B* **58**(20): 14013-14019.

Li, C. Y.; Chou, T. W. (2005): Axial and radial thermal expansions of single-walled carbon nanotubes. *Physical Review B* **71**(23): 6.

Liu, P.; Zhang, Y. W. et al. (2005): Atomistic simulations of formation and stability of carbon nanorings. *Physical Review B* **72**(11).

Liu, P.; Zhang, Y. W. et al. (2005): Structures and stability of defect-free multiwalled carbon toroidal rings. *Journal of Applied Physics* **98**(11):

Lourie, O.; Wagner, H. D. (1998): Evaluation of Young's modulus of carbon nanotubes by micro-Raman spectroscopy. *Journal of Materials Research* **13**(9): 2418-2422.

Lu, J. P. (1997): Elastic properties of carbon nanotubes and nanoropes. *Physical Review Letters* **79**(7): 1297-1300.

Lu, J. P. (1997): Elastic properties of single and multilayered nanotubes. *Journal of Physics and Chemistry of Solids* **58**(11): 1649-1652.

Maniwa, Y.; Fujiwara, R. et al. (2001): Thermal expansion of single-walled carbon nanotube (SWNT) bundles: X-ray diffraction studies - art.no. 241402. *Physical Review B* **64**(24): 3.

Monkhorst, H. J.; Paack, J. D. (1976): Special Points For Brillouin-Zone Integrations. *Phys. Rev. B* **13**: 5188.

Nasdala, L.; Ernst, G. et al. (2005): Finite element analysis of carbon nanotubes with stone-Wales defects. *CMES: Computer Modeling in Engineering & Sciences* **7**: 293-304.

Payne, M. C.; Teter, M. P. et al. (1992): Iterative Minimization Techniques For Abinitio Total-Energy Calculations - Molecular-Dynamics And Conjugate Gradients. *Rev. Mod. Phys.* **64**: 1045.

Perdew, J. P.; Burke, K. et al. (1996): Generalized gradient approximation made simple. *Phys. Rev. Lett.* **77**: 3865.

Pop, E.; Mann, D. et al. (2006): Thermal conductance of an individual single-wall carbon nanotube above room temperature. *Nano Letters* **6**(1): 96-100.

Popov, V. N.; Van Doren, V. E. et al. (2000): Elastic properties of single-walled carbon nanotubes. *Physical Review B* **61**(4): 3078-3084.

Reich, S.; Thomsen, C. et al. (2002): Elastic properties of carbon nanotubes under hydrostatic pressure. *Physical Review B* **65**(15):

Robertson, D. H.; Brenner, D. W. et al. (1992): Energetics of Nanoscale Graphitic Tubules. *Physical Review B* **45**(21): 12592-12595.

Ruoff, R. S.; Tersoff, J. et al. (1993): Radial Deformation Of Carbon Nanotubes By Van-Der-Waals Forces. *Nature* **364**(6437): 514-516.

Tchouikov,S.; Nishioka, T. et al. (2005): Numerical Prediction of Dynamically Propagating and Branching Cracks Using Moving Finite Element Method. *CMC: Computers Materials & Continua* **1**(2): 191-204.

Salvetat, J. P.; Briggs, G. A. D. et al. (1999): Elastic and shear moduli of single-walled carbon nanotube ropes. *Physical Review Letters* **82**(5): 944-947.

Sanchez-Portal, D.; Artacho, E. et al. (1999): Ab initio structural, elastic, and vibrational properties of carbon nanotubes. *Physical Review B* **59**(19): 12678-12688.

Shen, S.; Atluri, S. N. (2004): Computational Nano-mechanics and Multi-scale Simulation. *CMC: Computers Materials & Continua* **1**(1): 59-90.

Srivastava, D.; Wei, C. et al. (2003): Nanome-

chanics of carbon nanotubes and composites. *Applied Mechanics Reviews* **56**(2): 215 - 230.

Theodosiou, T. C.; Saravanos, D. A. (2007): Molecular mechanics based finite element for carbon nanotube modeling. *CMES: Computer Modeling in Engineering & Sciences* **19**(2): 121-134.

Thostenson, E. T.; Ren, Z. F. et al. (2001): Advances in the science and technology of carbon nanotubes and their composites: a review. *Composites Science and Technology* **61**(13): 1899-1912.

Treacy, M. M. J.; Ebbesen, T. W. et al. (1996): Exceptionally high Young's modulus observed for individual carbon nanotubes. *Nature* **381**(6584): 678-680.

Tu, Z. C.; Ou-Yang, Z. (2002): Single-walled and multiwalled carbon nanotubes viewed as elastic tubes with the effective Young's moduli dependent on layer number. *Physical Review B* **65**(23):

van Lier, G.; Van Alsenoy, C. et al. (2000): Ab initio study of the elastic properties of single-walled carbon nanotubes and graphene. *Chemical Physics Letters* **326**(1-2): 181-185.

Wang, Y.; Wang, X. X. et al. (2004): Atomistic simulation of the torsion deformation of carbon nanotubes. *Modelling and Simulation in Materials Science and Engineering* **12**(6): 1099-1107.

Wong, E. W.; Sheehan, P. E. et al. (1997): Nanobeam mechanics: Elasticity, strength, and toughness of nanorods and nanotubes. *Science* **277**(5334): 1971-1975.

Xiao, J. R.; Gama, B. A. et al. (2005): An analytical molecular structural mechanics model for the mechanical properties of carbon nanotubes. *International Journal of Solids and Structures* **42**(11-12): 3075-3092.

Xie, G. Q.; Han, X. et al. (2007): Characteristic of waves in a multi-walled carbon nanotube. *CMC: Computers Materials & Continua* **6**(1): 1-11.

Xie, G. Q.; Long, S. Y. (2006): Elastic Vibration Behaviors Oof Carbon Nanotubes Based on Micropolar Mechanics. *CMC: Computers Materials & Continua* **4**(1): 11-20.

Yakobson, B. I.; Avouris, P. (2001): Mechanical Properties of Carbon Nanotubes. *Carbon Nanotubes: Synthesis, Structure, Properties, and Applications*. G. Dresselhaus, M. S. Dresselhaus and P. Avouris, Springer: 447.

Yakobson, B. I.; Brabec, C. J. et al. (1996): Nanomechanics of carbon tubes: Instabilities beyond linear response. *Physical Review Letters* **76**(14): 2511-2514.

Yu, M. F.; Files, B. S. et al. (2000): Tensile loading of ropes of single wall carbon nanotubes and their mechanical properties. *Physical Review Letters* **84**(24): 5552-5555.

Zhou, G.; Duan, W. H. et al. (2001): First-principles study on morphology and mechanical properties of single-walled carbon nanotube. *Chemical Physics Letters* **333**(5): 344-349.